DOI: 10.19884/j.1672-5220.202307003

Comparative Simulation Study of Active Sound Absorption Based on Piezoelectric Materials

ZHU Congyun[1*], CAO Haiyang[1], DING Guofang[1], HUANG Qibai[2]
1. School of Mechatronics Engineering, Zhongyuan University of Technology, Zhengzhou 450007, China
2. College of Mechanical Engineering, Huazhong University of Science and Technology, Wuhan 430074, China

Abstract: Active control simulation software is scarce, and most control problems are either computed using MATLAB programming or conducted through experimental setups. The former often yields unreliable simulation results, while the latter requires substantial financial resources. To address this issue, this article presents a new simulation method for comparing the active sound absorption and noise reduction performance of circular and square piezoelectric ceramic plates. The simulation method involves three steps. Firstly, ANSYS dynamic analysis is used to obtain the voltage generated by two polyvinylidene fluoride (PVDF) piezoelectric sensors on the piezoelectric ceramic plates under the current load step and separate the sound pressure and particle vibration velocity. Secondly, the sound pressure and particle velocity signals obtained in the first step are imported into MATLAB to separate the incident and reflected sound waves, and the optimal control algorithm in MATLAB is used to calculate the driving voltage to be applied. Thirdly, the driving voltage calculated by MATLAB is applied to both ends of the piezoelectric ceramic plates in ANSYS, and dynamic analysis is performed again to obtain the voltage generated by two PVDF piezoelectric sensors under the next load step. By repeating the above three steps, the active sound absorption control process of the piezoelectric ceramic plates can be simulated. The simulation experiment reveals the relationship between the applied driving voltage and frequency on piezoelectric ceramic plates of different shapes, and the simulation results closely match the theoretical calculations. The simulation experiment results demonstrate that, with the same surface area, circular piezoelectric ceramic plates exhibit significantly superior sound absorption and noise reduction performance compared to square piezoelectric ceramic plates.

Key words: active sound absorption; active control; piezoelectric material; ANSYS; MATLAB
CLC number: TB535+.2 **Document code:** A
Article ID: 1672-5220(2024)03-0308-07

Open Science Identity (OSID)

0 Introduction

Currently, considerable progress has been made in the research of passive sound absorption in the domestic field. Zhu et al.[1] proposed a new acoustic barrier structure composed of a resonant micro-perforated panel absorption structure and an impedance composite sound absorption structure. Zhu et al.[2] utilized the multi-physics simulation software COMSOL and employed the finite element method to study the acoustic characteristics of a direct-through perforated tube silencer with multiple layers of sound-absorbing materials. Zhang et al.[3] researched the combined active and passive sound absorption of porous panels. However, the research on active sound absorption is still relatively limited. The active noise control (ANC) proposed by Lueg et al.[4] in 1936, remained theoretical due to technological limitations at the time. With the development of modern electronic technology, ANC was put into practical use. The active structural acoustic control (ASAC) proposed by Guicking et al.[5] in 1984 controlled the vibration of the structure by directly controlling the input of the structure to achieve noise control. Leroy et al.[6] designed an active and passive sound absorption structure in 2011, composed of a polyvinylidene fluoride (PVDF) film and polyurethane foam, and studied it using an impedance matching method. The experimental results showed that the PVDF film played a major control role for low-frequency noise below 500 Hz, while high-frequency noise above 1 500 Hz was mainly passively absorbed by the polyurethane foam, and the noise between 500 Hz and 1 500 Hz was absorbed by a combination of active and passive methods. Xu[7] conducted active control research on controlling the modal vibration of automobile panels using piezoelectric materials and achieved a noise reduction effect of 2 dB for the driver's right ear. Zhu[8] used the delay method and piezoelectric control principle to establish an equivalent circuit model of piezoelectric active control and measured the sound absorption effect of

Received date: 2023-07-18
Foundation item: National Natural Science Foundation of China (No. 51705545)
* Correspondence should be addressed to ZHU Congyun, email: zcy711126@163.com
Citation: ZHU C Y, CAO H Y, DING G F, et al. Comparative simulation study of active sound absorption based on piezoelectric materials[J]. *Journal of Donghua University (English Edition)*, 2024, 41(3): 308-314.

piezoelectric ceramics as the main control element. The results showed that the sound absorption coefficient of the device reached above 0.9 in a range of 1 to 5 kHz. Suryakant[9] conducted research on the influence of adding effective plate damping in structural absorbers on transmission loss. By connecting resistors to the external circuit of thin piezoelectric bimorphs attached to a copper plate, piezoelectric shunting was implemented to increase the damping of the copper plate. Experimental results demonstrated that the piezoelectric shunt increased the proportion of absorbed power and reduced the proportion of reflected power, thereby enhancing the transmission loss in the structural absorber. Wang[10] investigated the tunability of locally resonant piezoelectric metamaterials (LRPM) in low-frequency underwater sound absorption. A theoretical model for underwater sound absorption based on LRPM was developed, and the tunable sound absorption characteristics and perfect absorption mechanism were analyzed from the perspective of effective materials. The theoretical results were in good agreement with the numerical results. The study revealed that a thin LRPM layer could achieve perfect sound absorption at the target low frequency and could be actively tuned by adjusting the resonant shunt circuit. Piezoelectric materials were used to replace sensors in active sound absorption devices due to their advantages such as small mass, wide frequency response range, fast response speed, and excellent electromechanical coupling performance. In terms of active noise reduction, there have been many successful applications using the sound elimination method. The application of using piezoelectric ceramics to suppress structural vibration and reduce structural sound radiation was also widespread, but the research on using piezoelectric materials to replace secondary sound sources was still in the preliminary stage. In this paper, the piezoelectric ceramic lead zirconate titanate PZT-5 was used as the active sound absorption material, and the active sound absorption and noise reduction performance of circular piezoelectric ceramic plate (CPCP) and square piezoelectric ceramic plate (SPCP) with the same area were compared. The smaller the reflected sound pressure, the better the active sound absorption performance. Therefore, the control equation for PZT-5 was calculated and derived using the acoustoelectric method, and the required driving voltage was obtained by substituting the condition of zero reflected sound pressure into the control equation of PZT-5.

1 Detection Principle of Piezoelectric Ceramic Sound Absorption and Theoretical Calculation of Driving Voltage

1.1 Active sound absorption model

It is assumed that the noise wave is harmonic and acts on the surface of the piezoelectric ceramic plate perpendicularly. Figure 1 shows a simple arrangement of two PVDF piezoelectric sensors and a piezoelectric ceramic plate[11].

In Fig. 1, U represents the voltage applied to the piezoelectric ceramic plate. The PVDF piezoelectric sensors and piezoelectric ceramic plate are arranged equidistantly with a distance of a. The noise wave is emitted from the left speaker, passes through two PVDF piezoelectric sensors, and reaches the left surface of the piezoelectric ceramic plate, producing reflected and transmitted sound waves. By controlling the driving voltage of the piezoelectric ceramic plate, the surface vibration velocities of the piezoelectric ceramic plate are made consistent with the vibration velocities of the air molecules on the surface of the piezoelectric ceramic plate.

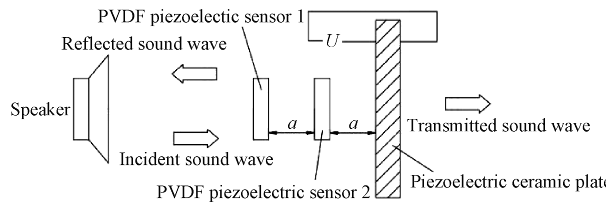

Fig. 1 Layout of piezoelectric ceramic plate and piezoelectric sensors

1.2 Extraction principle of incident sound pressure and reflected sound pressure

When pressure is applied to PVDF piezoelectric material, it undergoes a polarization effect, resulting in the generation of a potential difference on its surface. The mathematical model of the PVDF piezoelectric effect describes the relationship between the potential difference and the strain or pressure applied to the PVDF material, which can be expressed in the form of a mathematical equation:

$$U = \frac{X_d(Z_1 + Z_p)}{h_{33}\varepsilon_{33}^{s} Z_1} F, \tag{1}$$

where X_d represents the thickness of the PVDF piezoelectric sensor in the direction of polarization; Z_1 and Z_p respectively represent the acoustic impedance of air and the PVDF piezoelectric sensor; ε_{33}^{s} represents the dielectric constant of the PVDF piezoelectric sensor; h_{33} represents the voltage sensitivity constant of the PVDF piezoelectric sensor; F represents the pressure applied to the surface of the PVDF piezoelectric sensor.

Assuming the incident sound wave is a plane wave, the incident sound wave and the reflected sound wave can be represented as the function of displacement x and time t:

$$p_i(x,t) = P_i e^{j(\omega t - kx)}, \tag{2}$$

$$p_r(x,t) = P_r e^{j(\omega t + kx)}, \tag{3}$$

where k represents the wavenumber of the sound wave; ω represents the angular frequency of the sound wave; P_i represents the initial amplitude of the incident sound pressure; P_r represents the initial amplitude of the reflected sound pressure; j represents the imaginary unit.

According to the one-dimensional wave equation, it can be deduced that the planar sound pressure at the positions of PVDF piezoelectric sensor 1 and PVDF piezoelectric sensor 2 is a superposition of the incident and reflected sound pressures, thus enabling sound pressure measurement at these two locations. Specifically, the sound pressure measured at PVDF piezoelectric sensor 1 and PVDF piezoelectric sensor 2 can be expressed as

$$p_1(0,\ t) = p_i(0,\ t) + p_r(0,\ t) = P_i e^{j\omega t} + P_r e^{j\omega t}, \tag{4}$$

$$p_2(a,\ t) = p_i(a,\ t) + p_r(a,\ t) = P_i e^{j(\omega t - ka)} + P_r e^{j(\omega t + ka)}. \tag{5}$$

By taking the left side of PVDF piezoelectric sensor 1 as the coordinate origin and the positive half-axis of the x-axis as the direction to the right, the above formula can be used for calculation and separation of the incident sound pressure p_i and the reflected sound pressure p_r as

$$p_i = \frac{p_1 e^{-jka} - p_1}{e^{j\omega t}(e^{-2jka} - 1)}, \tag{6}$$

$$p_r = \frac{p_2 e^{jka} - p_1}{e^{j\omega t}(e^{2jka} - 1)}. \tag{7}$$

In theoretical calculations, the above formula can be used to obtain the incident and reflected sound pressure. However, due to the presence of complex exponential functions in the formula and the limited capability of ANSYS in calculating complex exponential functions, it is necessary to modify the formula to make it compatible with the simulation software.

The one-dimensional acoustic wave equation is

$$\rho \frac{\partial v}{\partial x} + \frac{\partial p}{\partial x} = 0, \tag{8}$$

where ρ is the air density; v is the propagation velocity of sound waves in air; p is sound pressure.

When the distance between two piezoelectric sensors is relatively small compared to the wavelength of the sound wave, it can be approximated as[12]

$$\frac{\partial p}{\partial x} = \frac{p_2 - p_1}{a}, \tag{9}$$

where p_1 and p_2 denote the sound pressures collected at the position of two piezoelectric sensors.

The vibration velocities of the incident sound wave and the reflected sound wave, v_i and v_r, are expressed as

$$v_i = \frac{1}{\rho c} p_i, \tag{10}$$

$$v_r = -\frac{1}{\rho c} p_r, \tag{11}$$

where c represents the speed of sound.

At the same time, the particle velocity can be obtained:

$$v(t) = \frac{1}{\rho a}\int_0^t (p_i - p_r)\,dt. \tag{12}$$

Considering the small distance between the two sensors, the sound pressure and particle velocity at the midpoint of the sensor can be approximated as

$$p = (p_1 + p_2)/2 = p_i + p_r, \tag{13}$$

$$v = v_i + v_r = (p_i - p_r)/\rho c. \tag{14}$$

According to the above formula, the incident sound pressure and the reflected sound pressure can be obtained as

$$p_i = (p + \rho c v)/2, \tag{15}$$

$$p_r = (p - \rho c v)/2. \tag{16}$$

1.3 Piezoelectric material sound absorption principle

A simple schematic diagram of the piezoelectric ceramic plate is shown in Fig. 2, where F_1 and F_2 respectively represent the external forces applied in the polarization directions of the piezoelectric ceramic plate; d represents the thickness of the piezoelectric ceramic plate; S represents the polarized area on the surface of the piezoelectric ceramic plate; v_1 and v_2 represent the vibration velocities in the polarization directions of the piezoelectric ceramic plate; U represents the voltage produced at the two ends of the piezoelectric ceramic plate.

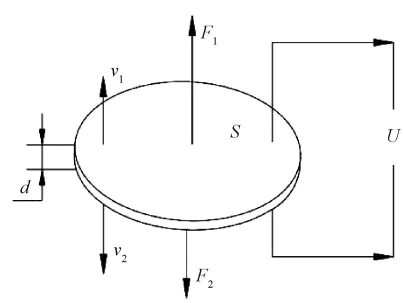

Fig. 2 Simplified diagram of piezoelectric ceramic plate

According to the acoustic boundary conditions, it can be obtained:

$$F_1 = (p_i + p_r) \times S, \tag{17}$$

$$v_1 = (p_i - p_r)/Z_1, \tag{18}$$

$$F_2 = p_t \times S, \tag{19}$$

$$v_2 = -p_t/Z_1, \tag{20}$$

where p_t represents the transmitted sound wave.

The polarization direction of the piezoelectric ceramic plate is oriented perpendicular to its surface, while the direction perpendicular to the polarization direction is isotropic. We consider only the case of one-dimensional harmonic sound waves incident in the direction perpendicular to the surface of the piezoelectric ceramic plate. The piezoelectric ceramic plate is only disturbed in the direction of its thickness.

According to the reference, there exists the following relationship:

$$(S+W)p_i+(S-W)p_r=\frac{Z_{e2}}{Z_1}p_t+MI, \qquad (21)$$

$$MI+p_i\frac{Z_{e2}}{Z_1}=\frac{Z_{e2}}{Z_1}p_r+(S-W)p_t, \qquad (22)$$

$$\frac{M}{B}I+\frac{B}{Z_1}p_i=\frac{B}{Z_1}p_r-\frac{B}{Z_1}p_t+U, \qquad (23)$$

where Z_e is electrical impedance; $W=(Z_{e1}+Z_{e2})/Z_1$; $Z_{e1}=\mathrm{j}S\rho_p C_a\tan\frac{kt}{2}$; $Z_{e2}=\frac{-\mathrm{j}S\rho_p C_a}{\sin(kt)}$; $M=\frac{B}{\mathrm{j}\omega C_a}$; $C_a=\frac{S\varepsilon_{33}{}^{s}}{d}$; $B=\frac{Se_{33}}{d}$; ρ_p represents the density of the piezoelectric ceramic plate; C_a represents the propagation velocity of acoustic waves in the piezoelectric ceramic plate; e_{33} represents the piezoelectric coupling coefficient of the piezoelectric ceramic plate.

According to formula (21), (22) and (23), we can get

$$\begin{pmatrix}p_t\\p_r\\I\\U\end{pmatrix}=p_i\begin{pmatrix}\frac{Z_{e2}}{Z_1} & W-S & M & 0\\ S-W & \frac{Z_1}{Z_{e2}} & -M & 0\\ \frac{B}{Z_1} & -\frac{B}{Z_1} & \frac{M}{B} & 1\end{pmatrix}^{-1}\begin{pmatrix}S+W\\ \frac{Z_{e2}}{Z_1}\\ -\frac{B}{Z_1}\end{pmatrix}. \qquad (24)$$

Here, p_r is the performance index to be controlled.

1.4 Control principle

To meet the real-time control requirement, the linear quadratic optimal control algorithm[13] was selected. The objective function of the linear quadratic optimal control algorithm is

$$J=\frac{1}{2}\int_0^{\infty}[\boldsymbol{z}^{\mathrm{T}}(t)\boldsymbol{Q}\boldsymbol{z}(t)+\boldsymbol{u}^{\mathrm{T}}(t)\boldsymbol{R}\boldsymbol{u}(t)], \qquad (25)$$

where $\boldsymbol{Q}$ represents a positive semi-definite matrix; $\boldsymbol{R}$ represents a positive definite matrix; $z(t)=\begin{bmatrix}p_r(t)\\ \dot{p}_r(t)\end{bmatrix}$ is the state vector of the piezoelectric acoustic structure controller, composed of the reflected sound pressure and its derivatives in front of the piezoelectric ceramic plate; $\boldsymbol{u}(t)=\begin{bmatrix}u(t)\\0\end{bmatrix}$ is the control vector of the piezoelectric acoustic structure controller, composed of the driving voltage applied to the piezoelectric ceramic plate.

The acoustic absorption model of the piezoelectric ceramic plate in the commonly used format of state equations is expressed as

$$\dot{z}=\boldsymbol{A}z(t)+\boldsymbol{B}\boldsymbol{u}(t)+\boldsymbol{E}\boldsymbol{r}(t), \qquad (26)$$

$$\boldsymbol{y}(t)=\boldsymbol{C}z(t), \qquad (27)$$

where $\boldsymbol{r}(t)=\begin{bmatrix}p_i(t)\\ \dot{p}_i(t)\end{bmatrix}$ is the state vector of the piezoelectric acoustic structure controller, composed of the incident sound pressure and its derivatives in front of the piezoelectric ceramic plate; $\boldsymbol{A}$ and $\boldsymbol{B}$ are constant matrices determined by the piezoelectric ceramic sound absorbing structure; $\boldsymbol{E}$ is the disturbance matrix; $\boldsymbol{C}$ is the gain matrix, where $\boldsymbol{C}=[10]$, meaning that only the reflected sound pressure is output; $\boldsymbol{y}(t)$ represents the system's output.

Since the reflected sound wave is controlled by the driving voltage applied at both ends of the piezoelectric ceramic plate, the input that the system needs to control is the driving voltage input when minimizing the objective function (25):

$$\boldsymbol{u}(t)=-\boldsymbol{G}z(t), \qquad (28)$$

where $\boldsymbol{G}$ is the feedback gain matrix.

The solution of $\boldsymbol{u}(t)$ can be solved by using the minimum principle and introducing the multiplier vector $\boldsymbol{\lambda}$ to establish the Hamiltonian function:

$$\boldsymbol{H}=\frac{1}{2}[z^{\mathrm{T}}(t)\boldsymbol{Q}z(t)+\boldsymbol{u}^{\mathrm{T}}\boldsymbol{R}\boldsymbol{u}(t)]+\boldsymbol{\lambda}^{\mathrm{T}}(t)[\boldsymbol{A}z(t)+\boldsymbol{B}\boldsymbol{u}(t)+\boldsymbol{E}\boldsymbol{r}(t)], \qquad (29)$$

$$\boldsymbol{\lambda}(t)=\boldsymbol{M}z(t), \qquad (30)$$

where $\boldsymbol{M}$ represents the undetermined matrix.

$\boldsymbol{M}$ can be obtained by solving the equation:

$$\boldsymbol{M}\boldsymbol{A}+\boldsymbol{Q}+\boldsymbol{A}^{\mathrm{T}}\boldsymbol{M}-\boldsymbol{M}\boldsymbol{B}\boldsymbol{R}^{-1}\boldsymbol{B}^{\mathrm{T}}\boldsymbol{M}=0. \qquad (31)$$

Finally, the optimal control input rule can be obtained as

$$\boldsymbol{u}(t)=-\boldsymbol{R}^{-1}\boldsymbol{B}^{\mathrm{T}}\boldsymbol{M}z(t). \qquad (32)$$

The feedback gain matrix in eq. (28) can be obtained:

$$\boldsymbol{G}=\boldsymbol{R}^{-1}\boldsymbol{B}^{\mathrm{T}}\boldsymbol{M}. \qquad (33)$$

The schematic diagram of the active control of piezoelectric ceramics with state feedback is shown in Fig. 3, where $1/s$ represents integration.

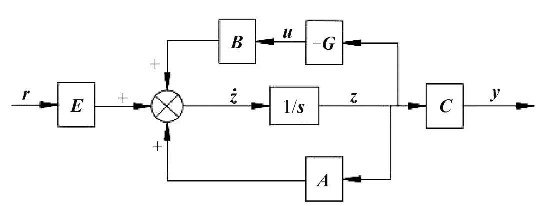

Fig. 3 Schematic diagram of active control

2 Simulation Experiment

The circular pipe with a diameter of 50 cm was used in the simulation experiment. The noise source was a planar sound wave emitted by a speaker with frequencies of 1 000, 2 000, 3 000, 4 000 and 5 000 Hz and a frequency amplitude of 1 Pa. The diameter of the CPCP was 29. 0 mm, and the thickness was 1. 5 mm, with the same surface area as the SPCP. The side length of the SPCP was 25. 7 mm, and the thickness was 1. 5 mm. The inner surface of the pipeline was set as a radiation boundary, and the sides of two piezoelectric ceramic plates were fixedly supported. The material parameters are shown in Table 1.

Table 1 Piezoelectric material parameters

Material	Density/ (kg/m^3)	Relative dielectric constant $\varepsilon_{33}^{s}/\varepsilon_0$	Piezoelectric stress constant/(C/m^2)	Elastic coefficient/ (N/m^2)	Propagation velocity of sound waves in piezoelectric materials/(m/s)
PZT-5	5 400	1 200	23. 3	3.9×10^8	4 540

The distance between PVDF piezoelectric sensor 1 and sensor 2, as well as between PVDF piezoelectric sensor 2 and the piezoelectric ceramic plate, was 2. 5 cm. When the speaker emitted sound waves, PVDF piezoelectric sensors 1 and 2 produced voltage due to the piezoelectric effect. The following steps were used to achieve simulated active control.

Step 1 Establish a structural model in the software SOLIDWORKS and import the model into ANSYS, apply noise waves, and impose boundary conditions and constraints.

Step 2 Perform dynamic analysis to obtain the voltage signals of two PVDF piezoelectric sensors under the influence of the noise wave.

Step 3 Use the time-delay method in MATLAB to separate the incident sound waves and the reflected sound waves at the positions of the two PVDF piezoelectric sensors.

Step 4 Use the optimal control algorithm that comes with MATLAB to solve the optimal driving voltage.

Step 5 Apply the calculated optimal driving voltage to both ends of the piezoelectric ceramic plates.

Step 6 Conduct dynamic analysis again to obtain the voltage signals of the two PVDF piezoelectric sensors.

The loading duration of each step is 1/20 of the period of the noise wave. The process of steps 2 to 6 can be repeated to achieve active control of sound absorption using the piezoelectric ceramic plates.

The simulation process is shown in Fig. 4.

An active noise control simulation model in ANSYS based on Fig. 1 is created, as shown in Fig. 5. In Fig. 5 (a), the leftmost component is a speaker, while the two square thin plates in the center-right position represent simulated PVDF piezoelectric sensors. On the far right, there is a piezoelectric ceramic plate, surrounded by a cylindrical enclosure. Figure 5 (b) shows a sectional view of the model rotated at an angle.

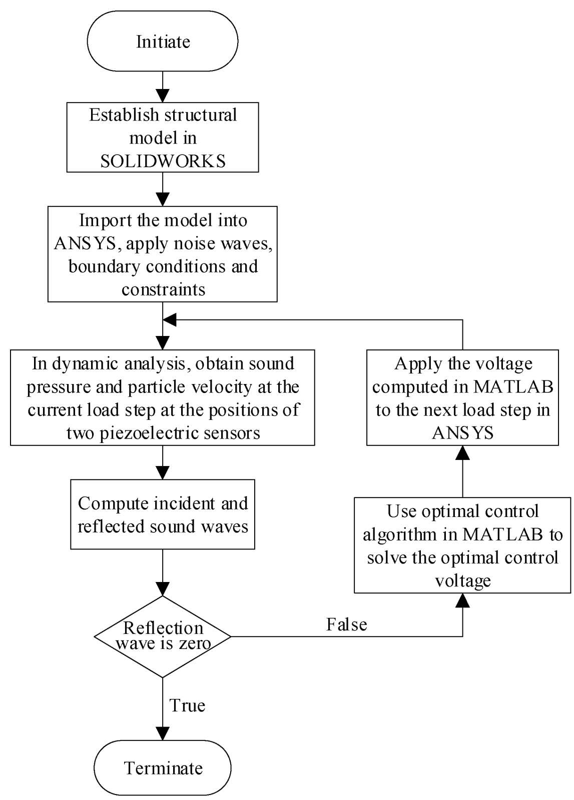

Fig. 4 Simulation flow chart

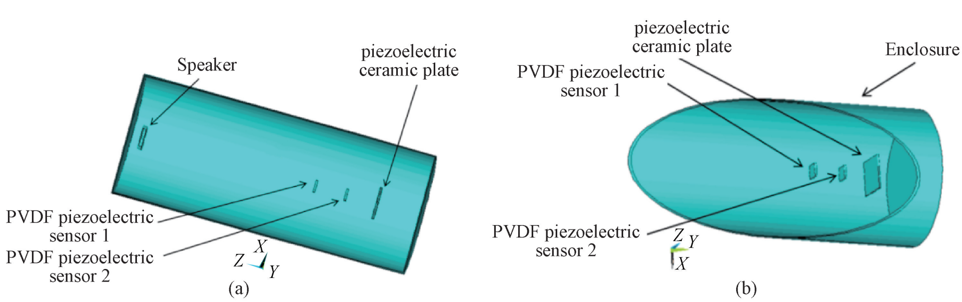

Fig. 5 Simulation model diagram: (a) vertical view; (b) sectional view at an angle

Figure 6 shows the experimentally obtained and theoretically calculated driving voltage phase values for both CPCP ans SPCP. It can be observed that the experimental values are greater than the theoretical values, and as the frequency increases, the difference in the driving voltage phase between them gradually increases.

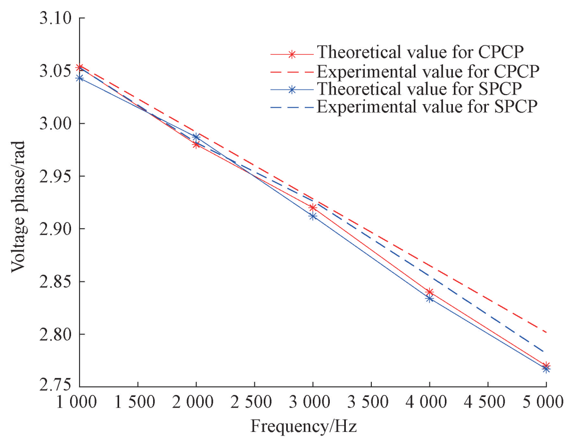

Fig. 6 Voltage phases of experimental value and theoretical value for both CPCP and SPCP

In Fig. 7, from the comparison of the experimentally obtained and theoretically calculated driving voltage amplitudes, it can be observed that the experimental values are lower than the theoretical values. As the frequency increases, such difference in driving voltage amplitudes gradually decreases. Furthermore, SPCP requires a lower driving voltage amplitude compared to CPCP.

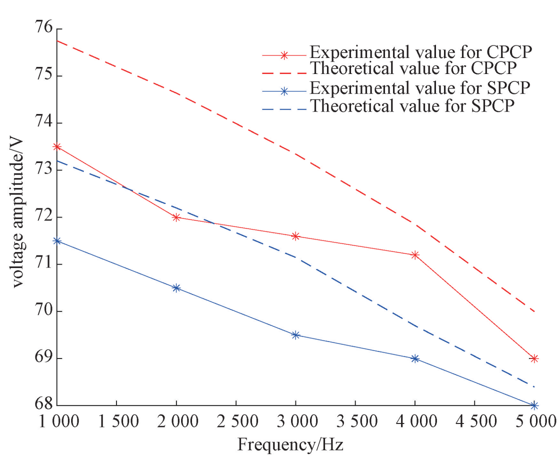

Fig. 7 Voltage amplitudes of experimental value and theoretical value for CPCP and SCPCP

Based on the sound pressure comparison of the PVDF piezoelectric sensor 2 before and after control in Figs 8 and 9, it can be observed that the sound pressure amplitude of the PVDF piezoelectric sensor 2 is below 1. 2 Pa and the sound absorption coefficient is around 0. 8 after control. This indicates that the applied driving voltage can fully control the reflected sound pressure of the piezoelectric material. In addition, CPCP exhibits better sound absorption performance than SPCP.

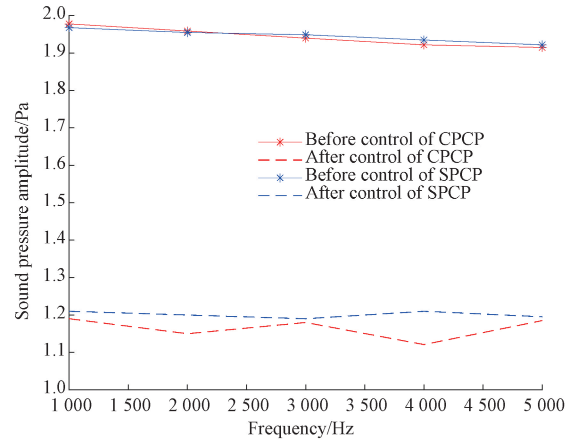

Fig. 8 Sound pressure amplitudes before and after control for both CPCP and SPCP

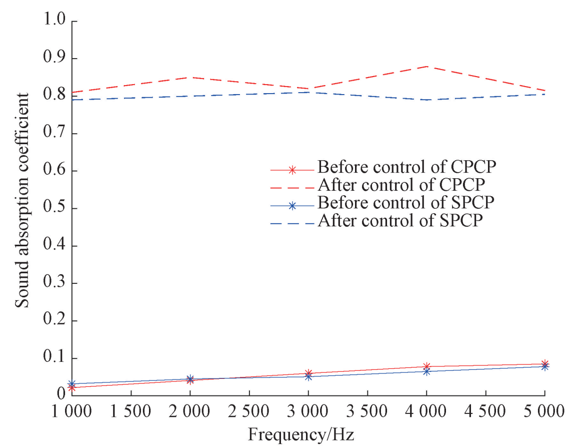

Fig. 9 Sound absorption coefficients before and after control for both CPCP and SPCP

3 Conclusions

Active sound absorption and noise reduction of the piezoelectric ceramic plate were simulated and controlled through a joint simulation experiment using ANSYS and MATLAB. The experimentally obtained driving voltage values were compared with the theoretically calculated values, and the results were close to the theoretical predictions. Furthermore, a comparison of the sound absorption effects before and after the control was conducted. These findings demonstrate that the joint simulation approach using ANSYS and MATLAB is effective for analyzing the active sound absorption of piezoelectric ceramic plates.

References

[1] ZHU C Y, WU R, HUANG P X, et al. Sound character calculation and analysis of sound barrier

based on acoustoelectric analogy[J]. *Journal of Donghua University (English Edition)*, 2019, 36(4): 369-376.

[2] ZHU C Y, LIU R J. Theoretical calculation and analysis of muffler based on multilayer sound absorbing material [J]. *Journal of Donghua University (English Edition)*, 2022, 39(1): 40-54.

[3] ZHANG R Q, ZHU C Y, DING G F, et al. Active absorption of perforated plate based on airflow [J]. *Journal of Donghua University (English Edition)*, 2022, 39(6): 590-596.

[4] LUEG P. Process of silencing sound oscillations. US, 2043416[P]. 1936-06-09.

[5] GUICKING D, KARCHER K. Active impedance control for one-dimensional sound[J]. *Journal of Vibration and Acoustics*, 1984, 106(3): 393-396.

[6] LEROY P, BERRY A, HERZOG P, et al. Experimental study of a smart foam sound absorber [J]. *The Journal of the Acoustical Society of America*, 2011, 129(1): 154-164.

[7] XU Z J. Research on active control for vehicle interior noise based on piezoelectric effect[D]. Shanghai: Shanghai University of Engineering Science, 2017. (in Chinese)

[8] ZHU C Y. Research on theories and methods of active sound absorption[D]. Wuhan: Huazhong University of Science and Technology, 2004. (in Chinese)

[9] SURYAKANT C N, SINGH A, RAMDAS R, et al. Enhanced absorption in structural acoustic silencers using piezo-shunting[J]. *The Journal of the Acoustical Society of America*, 2022, 152(2): 1112-1122.

[10] WANG M F, YI K J, ZHU R. Tunable underwater low-frequency sound absorption via locally resonant piezoelectric metamaterials[J]. *Journal of Sound and Vibration*, 2023, 548: 117514.

[11] YANG D. Research on theories and methods of active absorption using piezoelectric composite structure[D]. Wuhan: Huazhong University of Science and Technology, 2010. (in Chinese)

[12] GUO Z Y. Theory of active noise absorption and methods of designing the control system[D]. Wuhan: Huazhong University of Science and Technology, 2012. (in Chinese)

[13] ZHU Y H, TANG W H. Research on linear quadratic regulator algorithm [J]. *Modern Navigation*, 2018, 9(6): 451-454. (in Chinese)

基于压电材料的主动吸声仿真方法研究

朱从云[1*]，曹海洋[1]，丁国芳[1]，黄其柏[2]

1. 中原工学院 机电学院，河南 郑州 450007

2. 华中科技大学 机械工程学院，湖北 武汉 430074

摘　要：主动控制仿真软件很少，大部分控制问题都采用 MATLAB 自编程进行计算或搭建试验台进行试验，前者仿真结果不可靠，后者需要消耗大量的经费。针对这种问题，该文采用一种新的仿真方法，对圆形和方形压电陶瓷片的主动吸声降噪性能进行对比研究。仿真步骤分三步。第一步，在 ANSYS 动态分析中获取压电陶瓷片前的两个聚偏氟乙烯（polyvinylidene fluoride，PVDF）压电传感器在当前载荷步下产生的声压和质点振动速度。第二步，将第一步得到的声压和质点振动速度信号导入 MATLAB，分离入射声波和反射声波，利用 MATLAB 自带的最优控制算法计算出需要施加的控制电压。第三步，在 ANSYS 中将 MATLAB 计算出的控制电压施加到压电陶瓷片的两端，再次进行动态分析，得到下一个载荷步的两个 PVDF 压电传感器产生的电压。重复以上三个步骤，就可以模拟出压电陶瓷片的主动吸声控制过程。仿真试验得到了施加在不同形状压电材料上的驱动电压与频率的关系，仿真结果与理论计算结果接近。仿真试验结果表明，在表面积相同的情况下，与方形压电陶瓷片相比，圆形压电陶瓷片的吸声降噪效果更显著。

关键词：主动吸声；主动控制；压电材料；ANSYS；MATLAB